ELSEVIER

Ultrasound in Med. & Biol., Vol. 24, No. 2, pp. 245–256, 1998
Copyright © 1998 World Federation for Ultrasound in Medicine & Biology
Printed in the USA. All rights reserved
0301-5629/98 $19.00 + .00

PII S0301-5629(97)00273-1

● *Original Contribution*

KINETICS OF THE "BLACK HOLE" PHENOMENON IN ULTRASOUND BACKSCATTERING MEASUREMENTS WITH RED BLOOD CELL AGGREGATION

ZHAO QIN,* LOUIS-GILLES DURAND* and GUY CLOUTIER*

*Laboratory of Biomedical Engineering, Institut de recherches cliniques de Montréal, Montréal, Canada; and Department of Medicine, University of Montreal, Montréal, Québec, Canada

(*Received* 17 *July* 1997; *in final form* 16 *October* 1997)

Abstract—The observation of a hypoechoic zone around the center of large tubes (the "black hole" phenomenon) in ultrasound backscattering measurements with red blood cell (RBC) aggregation was reported for the first time in 1989. Since then, a very limited number of studies tried to explain its complex mechanisms. In this study, blood models characterized by different RBC aggregation levels were prepared by diluting horse blood plasma with a saline solution in different proportions. A laser reflectometry technique was used to characterize the RBC aggregation kinetics and cohesion forces between RBCs for each blood sample. The blood was circulated in a 12.7 mm diameter vertical tube. For each experimental flow condition tested, 25 or 15 power Doppler ultrasound measurements were performed across the tube with a 10-MHz system and insonation angles varying between 40° to 70°. For flow rates varying between 100 and 1250 mL/min, the "black hole" was observed in most measurements performed with different aggregating RBC models. The "black hole" was more pronounced for RBCs with a high kinetics of aggregation and measurements with increasing Doppler angles. Previous studies suggested that this phenomenon is due to tube entrance effects, and the reduction of RBC aggregation at very low shear rates around the center of the tube. In the present study, the "black hole" was observed for shear rates up to 25 s^{-1}. It is suggested that the structural organization and orientation of RBC rouleaux may participate in the mechanism leading to the "black hole" phenomenon. A schematic representation of the rheological behavior of horse RBCs in a large tube under steady flow is presented. © 1998 World Federation for Ultrasound in Medicine & Biology.

Key Words: **Acoustic backscattering, Biofluid mechanics, Erythrocyte aggregation, Power Doppler ultrasound, "Black hole" phenomenon, Acoustic anisotropy, Biorheology, Model.**

INTRODUCTION

Red blood cell (RBC) aggregation exists in the normal blood circulation and is abnormally increased in patients with degenerative diseases, acute and chronic infections. The process of RBC aggregation is reversible and governed by the shear forces of the flow. In the presence of plasma adhesion macromolecules, a modal function describing the shear rate dependence of human RBC aggregation was first reported by Chien (1976) and Copley et al. (1976). According to these studies, the interaction between RBCs gets stronger and RBC aggregation is enhanced as the shear rate is increased from zero to 0.5 s^{-1}. For shear rates above 0.5 s^{-1}, the dispersion of human RBC aggregates begins and continues with increasing shear rates. At shear rates higher than approximately 50 s^{-1}, normal human RBC aggregates are almost completely disrupted. However, they will form again if the shear rate is reduced. Using ultrasound backscattering methods, the shear-rate dependence of RBC aggregation was studied *in vitro* (Sigel et al. 1983; Yuan and Shung 1988; Shehada et al. 1994; Van Der Heiden et al. 1995; Cloutier et al. 1996) and also *in vivo* (Sigel et al. 1982; Machi et al. 1983). The first observation of a hypoechoic hole at the center of a large tube with B-mode imaging is attributed to Yuan and Shung (1989).

Using a 7-MHz B-mode system, Mo et al. (1991) recorded images of porcine whole blood at 28% hematocrit for different entrance distances in a large diameter tube. From the images obtained at a constant mean flow velocity of 1.4 cm/s, they showed that the hypoechoic

Address correspondence to: Dr. Guy Cloutier, Laboratory of Biomedical Engineering, Institut de recherches cliniques de Montréal, 110 avenue des Pins Ouest, Montréal, Québec H2W 1R7 Canada. E-mail: cloutig@ircm.umontreal.ca

zone in the central axis of the tube appeared when increasing the inlet length of the tube. They suggested that the "black hole" arose from disaggregated RBCs that had insufficient time to reaggregate when they reached a steady state at the center of the tube. The relationship between RBC aggregation and the development of the "black hole" in B-mode ultrasound images was further studied by Shehada et al. (1994). A hypoechoic central zone with a surrounding hyperechoic ring that was dependent on the mean flow velocity was observed. They showed that the shear-rate dependence of porcine blood echogenicity followed a modal function. The hypoechoic central zone (the "black hole") corresponded to shear rates lower than 0.05 s^{-1}, and the surrounding hyperechoic ring to higher shear rates favorable for the enhancement of RBC aggregation (0.05 to 2 s^{-1}).

The objective of this study was to provide additional knowledge of the mechanisms of the "black hole". While studying the shear-rate dependence of horse blood models characterized by different levels of RBC aggregation (Cloutier and Qin 1997), the "black hole" phenomenon was observed in most measurements and over a wide range of flow rates. Based on the literature review and the results of the present study, it is hypothesized that, in addition to the modal relationship of the shear rate dependence of RBC aggregation and the dynamics of rouleau formation related to the entrance distance, the RBC rouleau orientation and their structural organization, as determined by the local distribution of the shear forces within the flow, may be additional factors contributing to the "black hole."

MATERIALS AND METHODS

Blood sample preparation

Horse blood was chosen for all experiments because of the requirement of large quantities of blood covering a wide range of aggregation levels. As described in Weng et al. (1996), by replacing different proportions of the total volume of plasma with an isotonic saline solution, different aggregation levels were obtained. The horse blood was collected from a local slaughterhouse. A solution of 1 g of EDTA in 10 mL of saline was immediately added to the blood at a concentration of 30 mL per liter of blood to prevent coagulation. Blood was then brought to the laboratory and stored at 4°C. All experiments were performed within 48 h after blood collection. Before each experiment, the plasma was separated from the red and white cells by sedimentation.

Measurements of RBC aggregation

Several blood samples of 1.5 mL were prepared by replacing a part (between 17% and 75%) of the total volume of plasma with an isotonic NaCl solution. Using a light-reflectometry technique based on a Couette flow arrangement (Erythroaggregameter, Regulest, Florange, France), RBC aggregation indices were measured from these samples at room temperature and 40% hematocrit. A laser diode (Hitachi, HL7801G) providing a radiation at 780 nm was used as the light source. Indices on RBC aggregation were derived from the analysis of the variation in light intensity of the signal scattered by blood, as described in Donner et al. (1988). Two series of measurements were performed by the instrument. In the first series, the blood sample was sheared for 10 s at 550 s^{-1} to provide rouleau disruption and RBC orientation with the flow. After abrupt cessation of the rotation, the variation of the scattered light intensity was recorded during the rouleau formation process. The instrument provided the following two indices on RBC aggregation kinetics: tA and S_{10} that correspond to the primary aggregation time and a mean kinetic index at 10 s, respectively. The parameter tA was obtained from the inverse of the slope of the scattered light intensity variation between 0.3 and 1.9 s after stoppage of the flow rotation. The index S_{10} was calculated as the ratio of the area above the light intensity curve during the first 10 s after flow stoppage to the total area during the same period of time. For the second series of measurements, the blood sample was sheared at 96 different levels from 6 to 720 s^{-1}. The scattered light intensity was recorded by the instrument as a function of the shear rate for each blood sample. The scattered signal was characterized by a light intensity increase up to a maximum, followed by a decay as the shear rate was raised. The partial dissociation threshold (γD) was obtained from the intersection of a regression line computed for shear rates below 20 s^{-1}, and a horizontal line intercepting the maximum of the scattered light intensity. The total dissociation threshold (γS) corresponds to the shear rate at the maximum scattered light intensity. These last two parameters provided information on the adhesive forces between RBCs. The values of S_{10}, γD and γS are proportional to the level of aggregation, whereas tA has an inverse relationship. The values of these parameters for normal human blood, pig, horse, sheep and calf bloods can be found in Weng et al. (1996).

According to the value of S_{10}, a dilution level was chosen to obtain the aggregation kinetics desired. A total of 14 experiments, each using a different aggregation level with S_{10} varying between 14.2 and 38.6, were performed. After the desired aggregation kinetics level was obtained for a specific experiment, 1.5 L of blood was reconstituted using the correct dilution level and circulated into the flow model for at least 1 half h before beginning the experiment. This procedure eliminated air bubbles and allowed the temperature of blood to reach that of the ambient air. The aggregation indices were

verified during the experiment from a sample of 1.5 mL taken from the flow model.

Experimental arrangement

The flow loop model used in the present study was described in detail in a previous paper by Cloutier et al. (1996). Briefly, this model is composed of a peristaltic pump, a vertical Kynar tube with an i.d. of 12.7 mm, a bottom reservoir of 2 L, and a top reservoir used to minimize the oscillations produced by the pump. A valve was used to control the flow rate and a cannulating-type flow probe was inserted into the flow tubing to measure the flow rate with an electromagnetic blood flowmeter (Cliniflow II, Carolina Medical Electronics, King, NC, model FM701D). A magnetic stirrer was used to continuously mix the blood in the bottom reservoir. The peristaltic pump circulated blood from the bottom to the top reservoir. To minimize the effect of the ultrasound attenuation along the beam path and to allow acoustic coupling, the Doppler probe operating at 10 MHz was immersed in a small tank filled with horse RBCs suspended in a saline solution at 40% hematocrit. A suspension of RBCs was used to avoid sedimentation of hyperaggregating cells. The pulse-repetition frequency (PRF) of the Doppler instrument was 19.5 kHz and the cut-off frequency of the high-pass wall filter was set at 3 Hz.

Measurements using different RBC aggregation levels

In the first part of the study, 4 experiments were performed using a wide range of RBC aggregation levels. The Doppler probe was fixed at an angle of 45° with respect to the tube axis and a total of 25 Doppler measurements were performed across the tube at incremental steps of 0.5 mm and flow rates varying between 100 and 1250 mL/min. All experiments were performed under laminar flow conditions. The spatial variation of the backscattered power across the tube allowed the observation of the "black hole." Measurements covered a distance of 8.5 mm in a direction perpendicular to the tube. The distance between the face of the transducer and the recording sites was fixed at 19 mm, which corresponded to a sample volume size of 3.7 mm^3 at −3 dB. For measurements at the center of the tube, the distance traveled by the sound wave was approximately the same in the tube and the tank filled with the horse RBC suspension.

For each of the 25 measurements performed across the tube, the mean velocity and the backscattered power were computed from the Doppler mean spectrum, as described in Cloutier et al. (1996). To determine the mean shear rate within the Doppler sample volume, the velocity profile across the tube was first fitted to the power law model:

$$v(r) = v_{max}[1 - (r/R)^n], \quad (1)$$

where v_{max} is the maximum centerline Doppler mean velocity, r is the distance from the center of the tube, R is the radius of the tube, and n is the power law exponent. The 25 velocity measurements and the extrapolated zero velocity values at the wall were used to fit this model. In a second step, a shear rate profile $\gamma(r)$ was obtained by calculating the derivative of $v(r)$:

$$\gamma(r) = nv_{max}r^{(n-1)}/R^n. \quad (2)$$

The shear rate within the Doppler sample volume was estimated by weighting the shear rate $\gamma(r)$ with a theoretical function describing the radial ultrasonic beam power pattern in the far-field of the transducer, as described in Cloutier et al. (1996). For all flow rates tested, the modal relationship of the Doppler power (or RBC aggregation) was obtained by expressing the power as a function of the shear rate within the Doppler sample volume.

Anisotropy of the "black hole" studied with hyperaggregating RBCs

In the second part of the study, 10 experiments using hyperaggregating RBCs were used to verify the

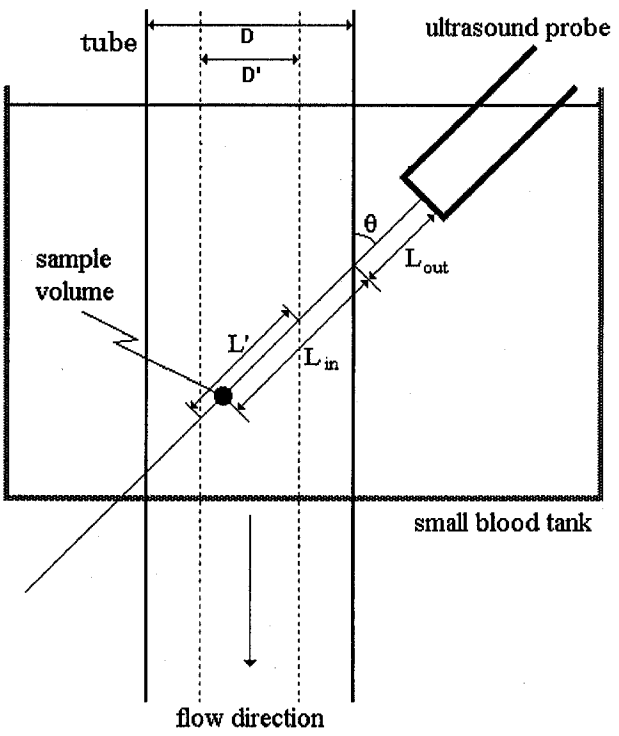

Fig. 1. Schematic representation of the positioning of the sample volume for measurements designed to characterize the anisotropy of the backscattered power.

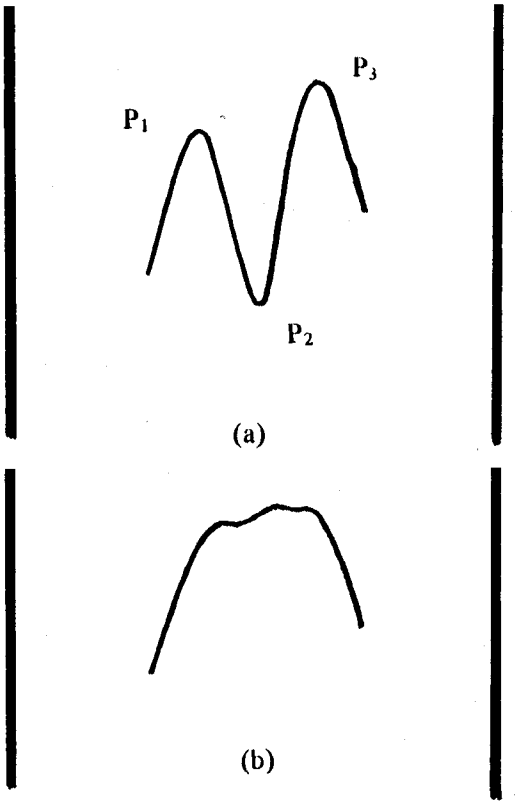

Fig. 2. Examples of the different forms of backscattered power variations obtained around the center of the tube: (a) a "black hole" with two power peaks P_1 and P_3 with different magnitudes; and (b) no identified "black hole."

hypothesis that the orientation of the RBC rouleaux is an important factor contributing to the "black hole" phenomenon. For this purpose, measurements were performed at Doppler angles varying between 40° and 70° by steps of 5°. Figure 1 illustrates the sample volume positioning for this part of the study performed at a constant flow rate of 1250 mL/min. An important factor had to be considered in this experimental protocol. By changing the Doppler angle, the refraction of the ultrasound beam at the wall of the tube could produce significant effects on the Doppler power backscattered by blood. Consequently, only relative power measurements were performed when changing the angle. In addition, because it is plausible to believe that the largest rouleaux are located around the center of the tube where the shear rate is low, only 15 measurements in the central region of the tube were performed for every angle tested. These 15 measurements covered a radial distance (D′) of 5.5 mm within the tube (see Fig. 1). To maintain D′ constant for all angles θ, the incremental displacement of the transducer (Δd) was modified when changing the insonating angle by using:

$$\Delta d = \frac{L'}{15} = \frac{D'}{15 \times \sin\theta}, \quad (3)$$

where L' is the distance covered within the tube at an angle θ.

It was experimentally observed that the attenuation of blood in the tube and that of the suspension of red cells surrounding the transducer were slightly different. To reduce this effect on the skewness of the backscattered power profile, the position of the transducer was adjusted to have $L_{in} = L_{out}$ (see Fig. 1) for the sample volume located at the center of the tube. At that position, the range gate was adjusted to maximize the Doppler frequency shift. By using this procedure, the backscattered power profiles were symmetrically skewed with respect to the tube center. To obtain $L_{in} = L_{out}$, the distance between the face of the transducer and the Doppler sample volume had to be changed for every angle tested. This distance was varied between 13.5 mm (70°) and 19.8 mm (40°). It corresponded to sample volume sizes varying between 3.0 and 4.0 mm^3 at −3 dB, respectively.

For each Doppler angle, the magnitude of the "black hole" was quantified by computing the difference between the maximum and the minimum power at the center of the tube obtained from the 15 measurements performed within the distance D′ (see Fig. 1). Because the "black hole" could be surrounded by two peaks having different amplitudes, as shown in Fig. 2a, its magnitude was estimated by using:

$$\text{Black hole magnitude} = 10 \times \log\left(\frac{P_1 + P_3}{2P_2}\right), \quad (4)$$

where P_1 and P_3 are the maximum power values observed on both sides of the central axis of the tube, and P_2 is the minimum power of the central hypoechoic zone. If no "black hole" was detected (see Fig. 2b), its magnitude was set to zero.

Table 1. Horse plasma dilution level and indices measured with the erythroaggregameter for a series of 4 experiments characterized by different RBC aggregation levels.

Number	Plasma dilution level (%)	S_{10}	tA (s)	γD (s^{-1})	γS (s^{-1})
1	17	38.6	1.37	61.1	470
2	50	29.3	1.77	–	>720
3	61	24.3	2.12	45.3	200
4	75	14.2	4.54	40.3	210

The instrument does not provide the value of γD when γS is >720.

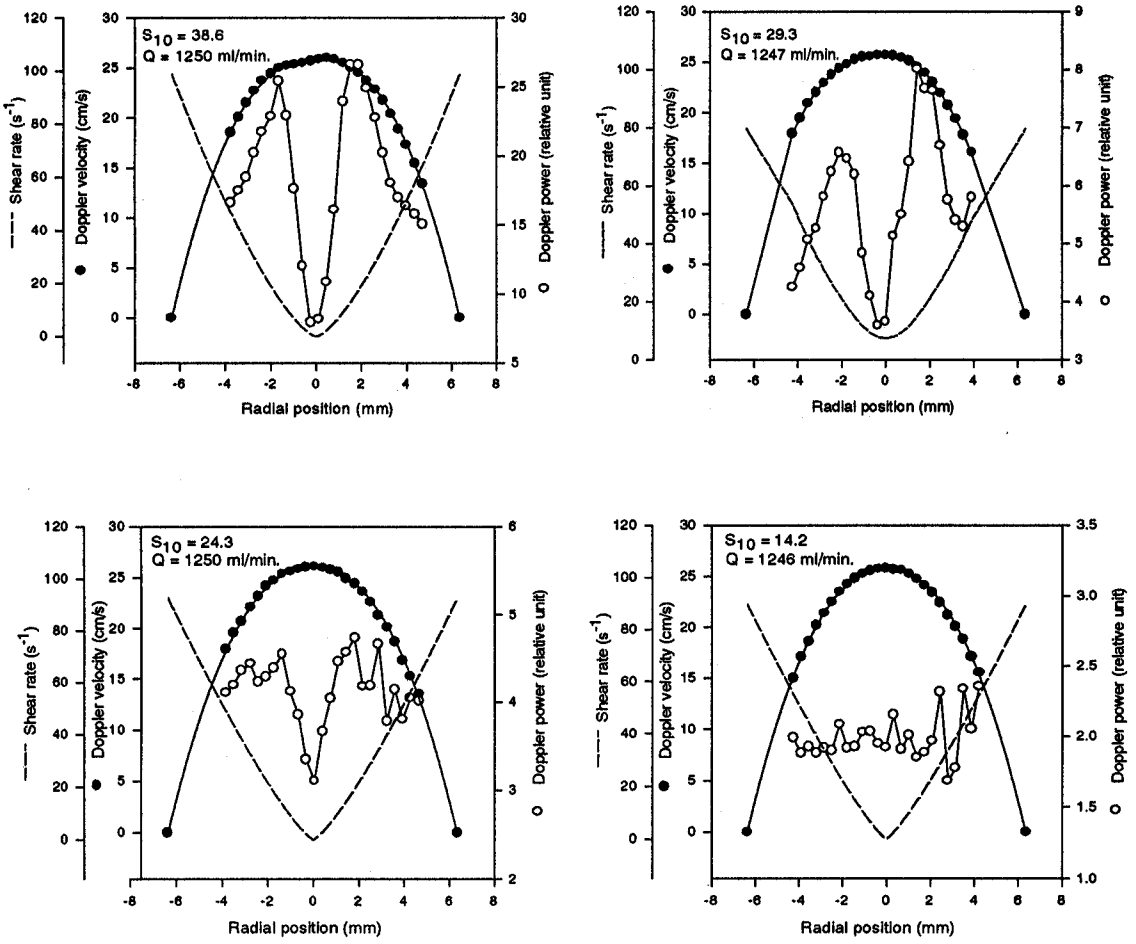

Fig. 3. Examples of Doppler mean velocity, Doppler backscattered power, and the fitted power law velocity model across the tube for a flow rate of 1250 mL/min approximately, and S_{10} varying between 14.2 and 38.6. S_{10} is the RBC aggregation kinetics index and Q is the flow rate.

RESULTS

The "black hole" phenomenon at different RBC aggregation levels

Table 1 summarizes the aggregation indices measured with the erythroaggregameter for this series of experiments. As observed, results for γD and γS were less consistent than those of tA and S_{10}.[1] By varying the mean flow rate between 100 and 1250 mL/min, the "black hole" was observed at the center of the tube for most measurements. Figure 3 shows examples of the distribution of the Doppler mean velocity, the Doppler power, the fitted power law velocity model, eqn (1), and the shear rate model, eqn (2), across the tube for a flow rate of approximately 1250 mL/min and S_{10} varying between 14.2 and 38.6. It can be observed that the reduction of the power at the center of the tube (the "black hole") was more important for hyperaggregating RBCs. For those measurements, the Doppler power was generally low near the wall, maximum between the wall and the center of the tube, and reduced at the central axis.

To better visualize the modal distribution of the Doppler backscattered power as a function of the shear rate and flow rate, the experimental data were fitted to log-normal functions (TableCurve,® Jandel Scientific, San Rafael, CA, version 1.10 for Windows®) and plotted using a logarithmic scale (dB), as shown in Fig. 4. For several measurements performed at different flow rates, the Doppler power in the tube increased when the shear rate was slightly higher than the lowest value measured. It then decreased when the shear rate was further in-

[1] This may be related to the fact that all measurements were performed at room temperature. In the study by Weng et al. (1996), diluting the plasma with an isotonic saline solution consistently reduced γD and γS at 37°C. Information on the reproducibility of the parameters measured with the erythroaggregameter can be found in Donner et al. (1988).

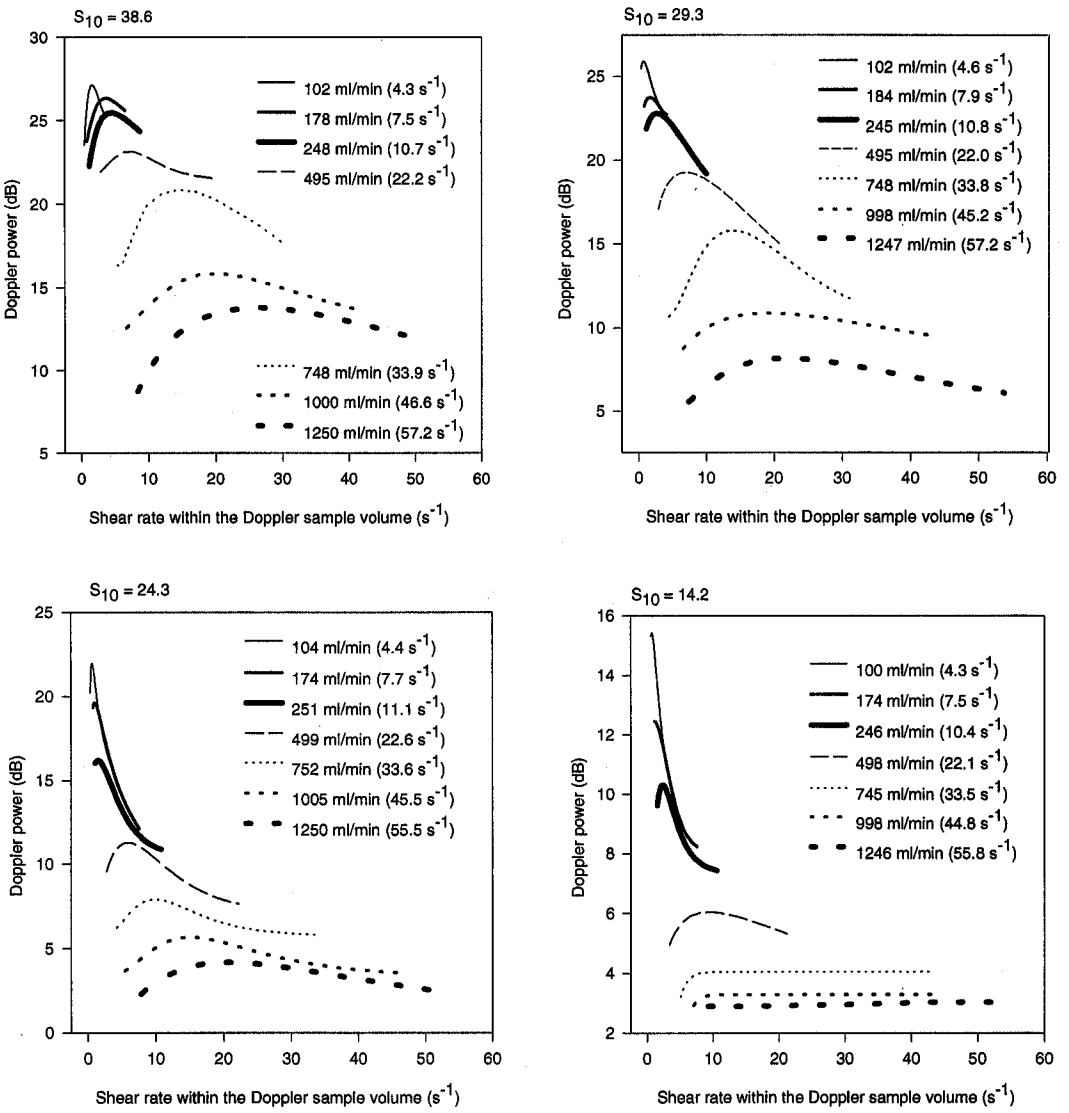

Fig. 4. Shear-rate dependence of the Doppler backscattered power in dB for S_{10} varying between 14.2 and 38.6, and flow rates varying between 100 and 1250 mL/min, approximately. S_{10} is the RBC aggregation kinetics index, and the numbers in parenthesis indicate the mean shear rate across the tube.

creased. For a given flow rate, measurements around the center of the tube corresponded to the left part of the log-normal function, and measurements toward the wall corresponded to the right part. The power increase at low shear rates, by up to 5 dB, is related to the magnitude of the "black hole" computed using eqn (4). With the exception of the experiment at S_{10} = 14.2, the peak of the Doppler power gradually decreased in magnitude and the shear rate at which the maximum power occurred gradually increased when the flow rate was raised. The shear rates corresponding to the maximum power values varied approximately from 1 to 25 s^{-1}, for flow rates varying between 100 and 1250 mL/min, approximately. The lack of power variations at high flow rates for S_{10} = 14.2 is due to the absence of rouleau build-up and disruption within the tube.

Anisotropy of the "black hole"

For this series of measurements, 10 trials were performed for each angle of insonation using horse blood having S_{10} around 34 (34.2 ± 1.5, n = 10). Figure 5 shows examples of Doppler mean velocities and Doppler power as a function of the position across the tube for different angles and S_{10} = 34.6. The magnitude of the "black hole" seemed to increase as the Doppler angle was raised. Figure 6 shows the magnitude of the "black hole" computed with eqn (4) as a function of the Doppler angle. Using a 1-way repeated measures analysis of

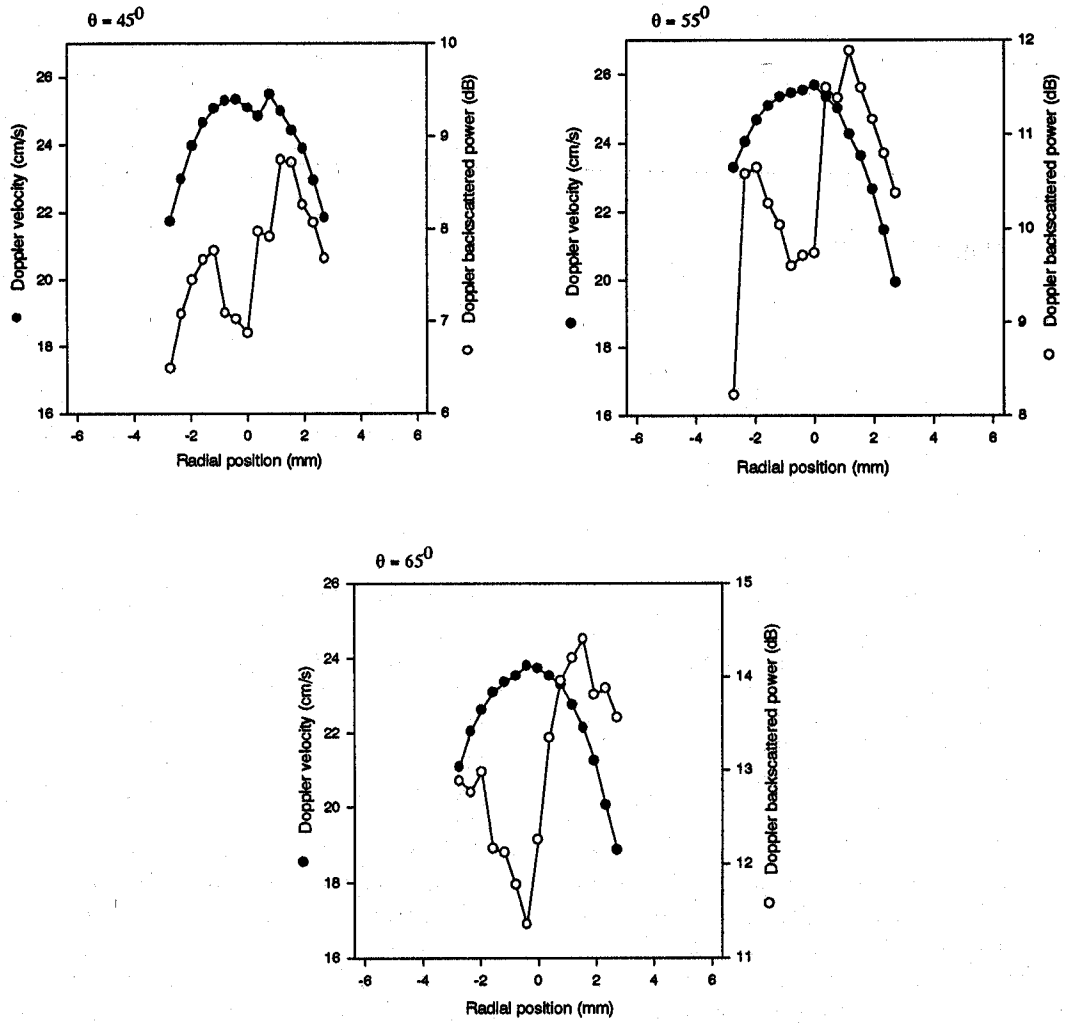

Fig. 5. Doppler velocity and Doppler power across the tube as a function of the Doppler angle θ for S_{10} of 34.6. The flow rate was approximately 1250 mL/min for all measurements. S_{10} is the aggregation kinetics index.

variance, the mean power variations shown in Fig. 6 were statistically significant ($p < 0.001$). The magnitude increased significantly between 40° and 65°, and dropped, not significantly, at 70°. The "black hole" had a mean magnitude of 1.0 dB at 40° and 2.1 dB at 65°. The anisotropic behavior of the Doppler power reduction at the center of the tube suggests that the orientation of rouleaux contributes to the magnitude of the "black hole."

DISCUSSION

The "black hole" phenomenon was observed for the first time in 1989 (Yuan and Shung 1989) and, since then, a very limited number of studies were oriented toward its explanation. As mentioned before, Shehada et al. (1994) proposed that the "black hole" and the hyperechoic ring around the hole result from the modal (log-normal) shear rate effect on porcine RBC aggregation. According to their experimental results, they suggested that the very low shear rates around the center of the tube ($< 0.05\ s^{-1}$) inhibit the formation of large rouleaux whereas higher shear rates (between 0.05 and 2 s^{-1}) in the surrounding region are favorable for the formation of aggregates producing the "bright ring." The entrance length was also shown to contribute to the "black hole" in the study by Shehada et al. (1994). For a given flow rate, the "black hole" was present only if sufficient time was allowed for the RBCs to form rouleaux in the higher echogenic ring.

In the present study with horse blood, the entrance length for all measurements was sufficient to allow rouleau build-up. Surprisingly, we observed Doppler power

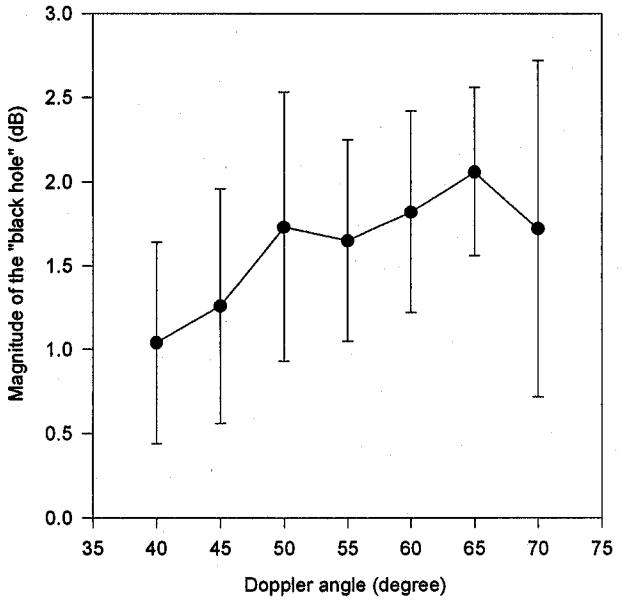

Fig. 6. Magnitude of the Doppler power reduction at the center of the tube ("black hole") as a function of the Doppler angle. The results are expressed in terms of mean ± SD and were averaged over 10 experiments. The mean aggregation kinetics index S_{10} was 34.2 ± 1.5 and the mean flow rate was 1250 mL/min, approximately.

drops at the center of the tube for almost all flow rates tested, and almost all blood samples characterized by different aggregation levels (see Figs. 3 and 4). It was also observed that the "black hole" is accentuated with hyperaggregating RBCs. Another interesting observation of the present study was the presence of the "black hole" at much higher velocities than those reported by Mo et al. (1991) and Shehada et al. (1994). For example, the velocity at the center of the tube in these studies was below 5.2 cm/s, but it ranged from 1.8 to 25.3 cm/s in our study. Another important difference was the shear rate at which the maximum backscattered power occurred for a given flow rate. In Shehada et al. (1994), the maxima were observed between 0.5 and 2 s^{-1} and they ranged from 1 to 25 s^{-1}, approximately, in our study (Fig. 4). Because it is unexpected that RBC aggregation might be enhanced at such high shear rates, we propose a new hypothesis explaining this finding after the following review on the behavior of rouleau structures in flowing blood and the anisotropy of ultrasound backscattering in tissues with longitudinal structures.

Rotations, deformations, and orientations of rouleaux of RBCs

Goldsmith and collaborators (Goldsmith and Mason 1966; Goldsmith and Marlow 1972; Goldsmith 1986) studied the flow behavior of rouleaux and elongated particles. Using normal human blood at low hematocrits circulating in small tubes with radii varying between 30 and 100 μm, they observed rotations and deformations of rouleaux in shear flow. During rotation, the angular velocity varied depending on the aggregate size. For rouleaux composed of 3 to 4 RBCs, the angular velocity was constant throughout the orbit. For rouleau sizes of more than 4 cells, the angular velocity increased when rouleaux bent for rotation and was minimum when they stretched and oriented their long-axis parallel to the flow direction. At a given local shear rate, the period of rotation through 360° increased with increasing axis ratio (length/diameter) for both rouleaux and rod-like particles at low concentrations. The fraction of time during each orbit spent in orientations close to the direction of flow increased with increasing axis ratio. In a study by Chen et al. (1995), morphological changes of RBC aggregates were observed as a function of shear stress. Human RBCs at 10% hematocrit were circulated in a rectangular flow chamber. By increasing the shear stress, the RBC rouleaux were stretched, then large rouleaux were broken into small rouleaux, which were then subjected to further stretching by shearing until they broke again into smaller ones.

Experimental observations at high particle concentrations have also been reported. Using a concentration of 50% ghost RBCs suspended in plasma, 4-cell rouleaux exhibited irregular rotations and deformations, even at low shear rates, because of particle crowding (Goldsmith 1971). In a study on the flow behavior of rigid spheres, rods and discs at concentrations for which particle interactions were expected (Karnis et al. 1966),[2] particles did not rotate in the plug flow region. Rods and disks were slightly tilted and symmetrically organized with respect to the central axis of the tube (see Fig. 7). Off-axis, near the wall, particles exhibited erratic rotations and radial displacements.

Anisotropy of ultrasound backscattering measurements

The ultrasonic anisotropic property of some biological tissues consisting of oriented structures, like muscle fibers, has been reported many times (Nassiri et al. 1979; Picano et al. 1985; Aygen and Popp 1987; Rubin et al. 1988; Madaras et al. 1988; Mottley and Miller 1988; Hoffmeister et al. 1995). It is currently believed that this anisotropy depends on the orientation of fibers with respect to the angle of insonation (Recchia et al. 1995). For fibers perpendicular to the insonation angle, the backscattered power is maximum, and it is minimum for fibers aligned with the ultrasound beam. Only a limited number of *in vitro* measurements were performed to

[2] In that study, the particle concentration was around 30% (Harry L. Goldsmith's personal communication).

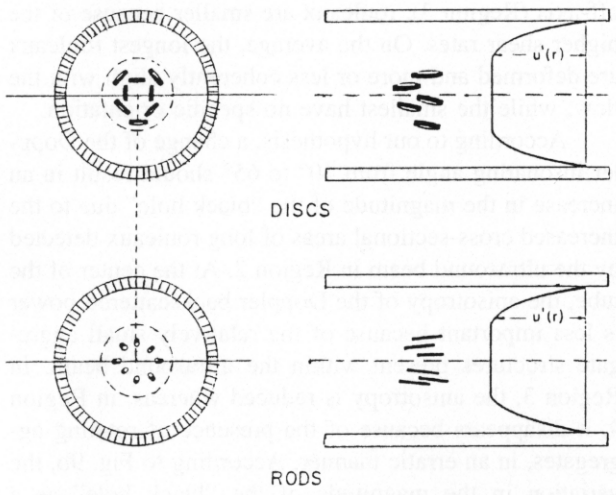

Fig. 7. Steady orientation of cylindrical particles viewed along the tube axis and in median plane in the region of plug flow in concentrated suspensions of discs and rods (schematic). In these experiments, the presence of a plug flow is due to particle crowding (Skalak 1992). Reproduced with permission from Karnis et al. (1966).

study the anisotropy of ultrasound backscattered by blood. Using a 10-MHz Doppler system, Allard et al. (1996) observed an angular dependence of the Doppler power at the center of the tube, for porcine whole blood circulated at mean shear rates varying from 17 to 51 s^{-1} across the tube. For a hematocrit of 40%, the maximum Doppler power was observed at insonation angles between 45° and 60°, suggesting a more tilted orientation of rouleaux than that of rigid rods presented in Fig. 7. In that study, no angular dependence was observed for saline suspensions of calf RBCs because they do not form rouleaux. Using a diluted suspension of carbon fibers, Allard et al. (1996) observed a strong anisotropy at the center of the tube. The backscattered power increased linearly by 8 dB for insonation angles varying from 40° to 80°. This anisotropic behavior suggests a more parallel orientation of carbon fibers with the flow compared to that of rouleaux of RBCs. Because of RBC crowding, porcine rouleaux at the center of the tube were probably free from rotation. On the other hand, most rotating carbon fibers were aligned within ± 10° with respect to the tube axis, on the average.

A new hypothesis explaining the genesis of the "black hole" phenomenon

Figure 8a, b, c shows photomicrographs, taken under static conditions, of normal and hyperaggregating human RBCs and horse blood. Horse RBCs were characterized by chains of rouleaux linked together to form large clusters, as also observed for hyperaggregating human RBCs. The orientation of these rouleaux is postulated as an additional factor intervening in the genesis of the "black hole" phenomenon. Because the magnitude

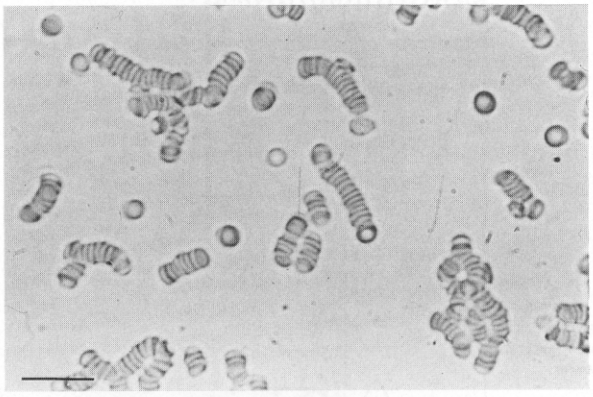

(a)

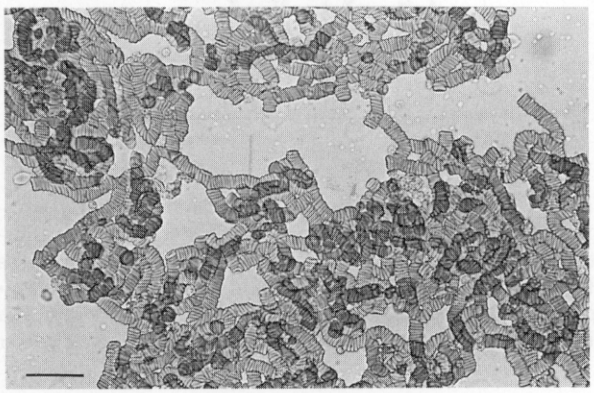

(b)

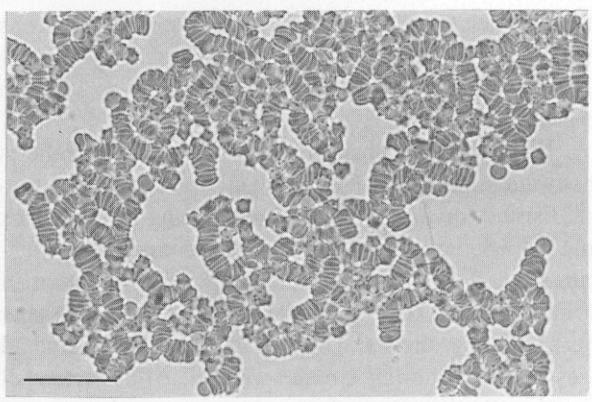

(c)

Fig. 8. Photomicrographs of (a) normal and (b) hyperaggregating human RBCs, and (c) horse blood under static conditions. The hyperaggregating human RBCs were obtained from a patient with a history of coronary artery disease. The horse blood model was obtained by replacing 67% of the total volume of plasma with an isotonic saline solution. Magnifications: (a) 375 X, (b) 330 X, (c) 480 X. The horizontal line on each panel corresponds to a distance of 30 μm.

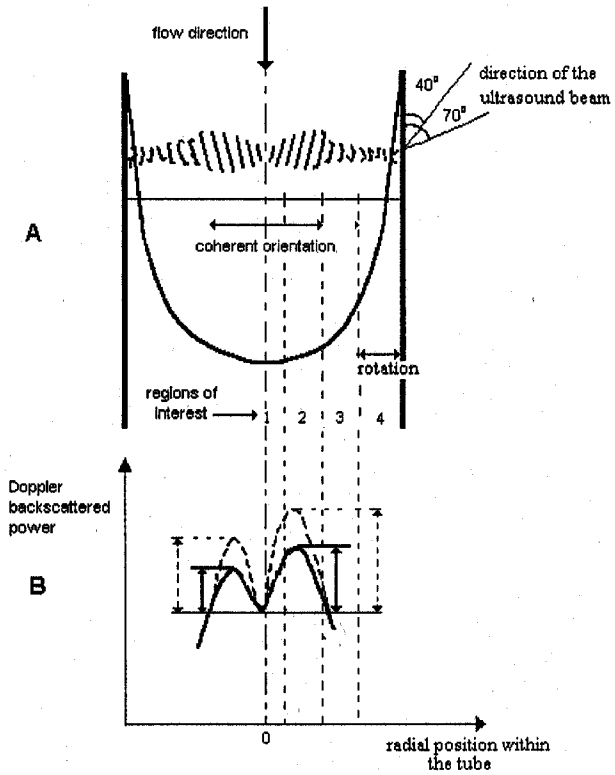

Fig. 9. (A) Schematic representation of the hypothesized macroscopic structural organization of RBC aggregates for different shear rates across the tube. (B) Postulated angular variations of the backscattered power. The solid and dotted lines correspond to Doppler angles of 40° and 65°, respectively. The bidirectional arrows represent the region with the largest power variations.

of the "black hole" increased as the Doppler angle was raised from 40° to 65°, rouleaux were probably symmetrically oriented at an angle of approximately ± 25° with respect to the tube axis.

Figure 9A, B illustrates the following hypothesis about the influence of RBC rouleau orientation and spatial distribution on the mechanism leading to the "black hole" phenomenon. In all our measurements, the entrance length was sufficient to allow the formation of various sizes of RBC aggregates. In the region of higher shear rates near the wall (Region 4), rouleaux have small sizes and bend during erratic rotations. At the center of the tube (Region 1), rouleaux do not rotate because of particle crowding and long chains are inhibited by the too small shear rates (Copley et al. 1976). The increased shearing off-axis (Region 2) enhances the probability of cell bridging leading to the formation of the largest nonrotating rouleaux. The high adhesive forces between RBCs for horse blood probably reduced the flexibility of rouleaux. This factor, particle crowding, and the presence of long rouleaux prevented rouleau rotation. Further off-axis (Region 3), rouleaux are smaller because of the higher shear rates. On the average, the longest rouleaux are deformed and more or less coherently align with the flow, while the smallest have no specific orientation.

According to our hypothesis, a change of the Doppler insonating angle from 40° to 65° should result in an increase in the magnitude of the "black hole" due to the increased cross-sectional areas of long rouleaux detected by the ultrasound beam in Region 2. At the center of the tube, the anisotropy of the Doppler backscattered power is less important because of the relatively small aggregate structures present within the ultrasound beam. In Region 3, the anisotropy is reduced whereas, in Region 4, it disappears because of the presence of rotating aggregates, in an erratic manner. According to Fig. 9b, the variation in the magnitude of the "black hole" as a function of the Doppler angle is due to changes in the backscattered power in the region where rouleaux are the largest and aligned together (see the bidirectional arrows).

As shown in Fig. 4, the flow rate strongly influences the magnitude of the Doppler backscattered power and the shape of the log-normal power distribution as a function of the shear rate. The decrease in the magnitude of the backscattered power is attributed to a decrease in rouleau sizes as the flow rate and the corresponding shear rate were increased. Indeed, large aggregates are more easily broken because of the higher mechanical fragility of long rouleaux. Figure 4 also shows that the shape of the Doppler power distribution changed with the flow rate. At the lowest flow rate, a narrow log-normal function was observed whereas it widened progressively with increasing flow rates. Moreover, the peak of the backscattered power was shifted to higher shear rates when the flow rate was increased. The well-organized structure of rouleaux, proposed in Fig. 9, was probably maintained at higher flow rates, but with smaller rouleaux. The high cohesion of this structure can explain the high shear rate of 25 s^{-1} needed to disrupt rouleaux at 1250 mL/min for hyperaggregating RBCs.

Based on the model of Fig. 9, a stronger backscattered power would have been expected from RBC rouleaux located on the left side of the tube because those rouleaux are aligned more perpendicular to the ultrasound beam. As seen in Figs. 3 and 5, the backscattered power was often skewed toward the right side instead of the left side of the tube. For measurements on the left side, the ultrasonic waves travelled a distance L_{in}, which is larger than L_{out} (see Fig. 1). The unexpected weaker backscattered power on the left side of the tube is probably due to the higher ultrasound attenuation in the moving blood with rouleaux, compared to that of the stationary suspension of nonaggregating RBCs in the reservoir containing the Doppler transducer.

Comparison with results obtained with porcine whole blood

According to a study by our group (Weng et al. 1996), porcine whole blood tends to produce clusters of RBCs instead of long chains of rouleaux at stasis. In the studies by Mo et al. (1991), Shehada et al. (1994), and Cloutier and Qin (1997), a "black hole" was detected with porcine whole blood. This finding may be explained, using our hypothesis, by the presence of clusters of small rouleaux at the center of the tube and oriented larger rouleaux off-axis at higher shear rates. It is important to mention here that our hypothesis is in agreement with the explanations provided by Mo et al. (1991) and Shehada et al. (1994). The mechanism proposed in the current study is complementary and more general. In a recent study by our group (Allard et al. 1996), backscattered power measurements were performed at the center of a tube at a Doppler angle varying between 40° and 80° to assess the anisotropy of porcine whole blood under conditions promoting RBC aggregation. Based on the observation of the angular dependence of the backscattered power, a cone-shaped orientation of rouleaux was postulated to be present at mean shear rates across the tube varying between 17 and 51 s^{-1}. It is interesting to note that this observation is also in agreement with our hypothesis illustrated in Fig. 9. At the lowest shear rates tested (8.5 s^{-1}) by Allard et al. (1996), large and complex clusters of aggregates were suggested to be present at the center of the tube, leading to the disappearance of the anisotropy.

CONCLUSION

The "black hole" phenomenon was observed in most backscattered power measurements reported in the present study. It was emphasized when using hyperaggregating equine RBCs and a Doppler angle of 65°. Previous studies suggested that this phenomenon is due to the reduction of RBC aggregation at very low shear rates and to tube entrance effects. Based on the present work, it is proposed that the structural organization of rouleaux across the tube and their orientation may contribute to the mechanism leading to the "black hole" phenomenon. A cone-shaped orientation of rouleaux was suggested to be present around the center of the tube under steady flow. The deformation of RBCs and stretching of rouleaux are other factors implicated in the rheology of blood in tube flow, although they were not specifically taken into consideration in the model of Fig. 9. The detection of the "black hole" phenomenon in human blood and its influence on the rheological properties of blood (like viscosity and flow resistance) has to be confirmed.

Acknowledgements—This work was supported by a research scholarship from the Fonds de la Recherche en Santé du Québec (G. C.), and by grants from the Medical Research Council of Canada (#MA-12491), the Whitaker Foundation, USA, and the Heart and Stroke Foundation of Québec. The authors gratefully acknowledge Dr. Harry L. Goldsmith for his helpful suggestions and guidance to the literature on the rheology of suspensions, Louis Allard for reviewing the manuscript, and abattoir du Richelieu, St-Aimé, Québec for providing us equine blood.

REFERENCES

Allard L, Cloutier G, Durand LG. Effect of the insonification angle on the Doppler backscattered power under red blood cell aggregation conditions. IEEE Trans Ultrason Ferroelec Freq Cont 1996;43:211–219.

Aygen M, Popp RL. Influence of the orientation of myocardial fibers on echocardiographic images. Am J Cardiol 1987;60:147–152.

Chen S, Gavish B, Zhang S, Mahler Y, Yedgar S. Monitoring of erythrocyte aggregate morphology under flow by computerized image analysis. Biorheology 1995;32:487–496.

Chien S. Electrochemical interactions between erythrocyte surfaces. Thromb Res 1976;8:189–202.

Cloutier G, Qin Z, Durand LG, Teh BG. Power Doppler ultrasound evaluation of the shear rate and shear stress dependences of red blood cell aggregation. IEEE Trans Biomed Eng 1996;43:441–450.

Cloutier G, Qin Z. Shear rate dependence of normal, hypo-, and hyper-aggregating erythrocytes studied with power Doppler ultrasound. In: Lees S, ed. Acoustical imaging. New York; Plenum Press, 1997;23:291–296.

Copley AL, King RG, Huang CR. Erythrocyte sedimentation of human blood at varying shear rates. In: Grayson J, Zingg W, eds. Microcirculation. New York: Plenum Press, 1976:133–134.

Donner M, Siadat M, Stoltz JF. Erythrocyte aggregation: Approach by light scattering determination. Biorheology 1988;25:367–375.

Goldsmith HL, Mason SG. Some model experiments in hemodynamics. III. In: Copley AL, ed. Hemorheology. Proceedings of the first international conference. New York: Pergamon Press, 1966:237–254.

Goldsmith HL. Deformation of human red cells in tube flow. Biorheology 1971;7:235–242.

Goldsmith HL, Marlow J. Flow behaviour of erythrocytes. I. Rotation and deformation in dilute suspensions. Proc Roy Soc (Lond) 1972; 182:351–384.

Goldsmith HL. The microcirculatory society Eugene M. Landis award lecture. The microrheology of human blood. Microvasc Res 1986; 31:121–142.

Hoffmeister BK, Wong AK, Verdonk ED, Wickline SA, Miller JG. Comparison of the anisotropy of apparent integrated ultrasonic backscatter from fixed human tendon and fixed human myocardium. J Acoust Soc Am 1995;97:1307–1313.

Karnis A, Goldsmith HL, Mason SG. The kinetics of flowing dispersions. I. Concentrated suspensions of rigid particles. J Colloid Interface Sci 1966;22:531–553.

Machi J, Sigel B, Beitler JC. Relation of in vivo blood flow to ultrasound echogenicity. J Clin Ultrasound 1983;11:3–10.

Madaras EI, Perez J, Sobel BE, Mottley JG, Miller JG. Anisotropy of the ultrasonic backscatter of myocardial tissue: II. Measurement in vivo. J Acoust Soc Am 1988;83:762–769.

Mo LYL, Yip G, Cobbold RSC, Gutt C, Joy M, Santyr G, Shung KK. Non-newtonian behavior of whole blood in a large diameter tube. Biorheology 1991;28:421–427.

Mottley JG, Miller JG. Anisotropy of the ultrasonic backscatter of myocardial tissue: I. Theory and measurements in vitro. J Acoust Soc Am 1988;83:755–761.

Nassiri DK, Nicholas D, Hill CR. Attenuation of ultrasound in skeletal muscle. Ultrasonics 1979;230–232.

Picano E, Landini L, Distante A, Salvadori M, Lattanzi F, Masini M, L'abbate A. Angle dependence of ultrasonic backscatter in arterial tissues: a study in vitro. Circulation 1985;72:572–576.

Recchia D, Hall CS, Shepard RK, Miller JG. Mechanisms of the view-dependence of ultrasonic backscatter from normal myocardium. IEEE Trans Ultrason Ferroelec Freq Cont 1995;42:91–98.

Rubin JM, Carson PL, Meyer CR. Anisotropic ultrasonic backscatter from the renal cortex. Ultrasound Med Biol 1988;14:507–511.

Shehada REN, Cobbold RSC, Mo LYL. Aggregation effects in whole blood: Influence of time and shear rate measured using ultrasound. Biorheology 1994;31:115–135.

Sigel B, Machi J, Beitler JC, Justin JR, Coelho JCU. Variable ultrasound echogenicity in flowing blood. Science 1982;218:1321–1323.

Sigel B, Machi J, Beitler JC, Justin JR. Red cell aggregation as a cause of blood-flow echogenicity. Radiology 1983;148:799–802.

Skalak R. An interpretation of partial plug flow of concentrated suspensions. Biorheology 1992;29:479–488.

Van Der Heiden MS, De Kroon MGM, Bom N, Borst C. Ultrasound backscatter at 30 MHz from human blood: influence of rouleau size affected by blood modification and shear rate. Ultrasound Med Biol 1995;21:817–826.

Weng XD, Cloutier G, Pibarot P, Durand LG. Comparison and simulation of different levels of erythrocyte aggregation with pig, horse, sheep, calf, and normal human blood, Biorheology 1996;33:365–377.

Yuan YW, Shung KK. Ultrasonic backscatter from flowing whole blood: I. Dependence on shear rate and hematocrit. J Acoust Soc Am 1988;84:52–58.

Yuan YW, Shung KK. Echoicity of whole blood. J Ultrasound Med 1989;8:425–434.